

Sternheimer Antishielding of the Fluorine Ion in Octahedral (MeF₆)⁴⁻-Complexes of Transition Metals from Perturbed Angular-Correlation Measurements

C. Bernhardt, F. W. Richter

Fachbereich Physik Universität Marburg (Lahn)

and

D. Babel

Fachbereich Chemie Universität Marburg (Lahn)

(Z. Naturforsch. **32a**, 1119–1125 [1977]; received August 4, 1977)

Sternheimer antishielding factors of fluorine in octahedral transition metal complexes have been determined from nuclear quadrupole coupling data derived from differential perturbed angular-correlation measurements taking into account ionic and covalent contributions to the electric field gradient at the fluorine nucleus. It has been found that the antishielding effect increases with increasing d-occupation in the metal ion, but is different for perovskite and rutile complexes and cannot be described by a scalar factor for the F⁻-ions in rutile fluorides, where the fluor position is of less than axial symmetry.

I. Introduction

Measurements of nuclear quadrupole interaction energies (NQI) give information about the product of the nuclear quadrupole moment Q times the electrical field gradient (EFG), which depends strongly on the environment of the nucleus under consideration.

By studying the quadrupole interaction of a certain nucleus in various chemical compounds the different charge-density distributions surrounding the nucleus are reflected by the experimental data^{1–3}. In ionic crystals which we are dealing with, there are various contributions to the EFG at a fixed lattice site: i) the EFG due to σ - and π -covalency; ii) the lattice EFG caused by the surrounding ions, which polarizes the considered ion and can lead to a large enhancement of the pure lattice EFG. This antishielding effect, firstly introduced by Sternheimer, is found to be — in first order — proportional to the lattice EFG in the case of closed shell ions¹. However, the agreement of antishielding factors derived from experimental data and those calculated by Sternheimer and others performed with free-ion wave functions is unsatisfactory^{4–8}. This is not surprising as pointed out by Sternheimer himself, since the wave function of an ion in a crystal will be significantly different from a free-ion wave function.

For the fluorine ion to which we shall refer, several free-ion Sternheimer correction factors

Table 1. Calculated Sternheimer-factor $(1 - \gamma_\infty)$ for the isolated Fluor-Ion F⁻.

Author	$(1 - \gamma_\infty)$
R. M. Sternheimer, H. M. Foley (1956) ¹	21.0
E. G. Wikner, T. P. Das (1958) ¹	22.03
R. E. Watson, A. J. Freeman (1961) ¹	21.15
G. Burns, E. G. Wikner (1961) ¹	22.22
R. Ingalls (1962) ¹	21.12
R. M. Sternheimer (1963) ¹	21.53
F. D. Feiock, W. R. Johnson (1969) ⁹	41.19

$(1 - \gamma_\infty)$ have been published (Table 1). They agree rather well, except the value of Feiock and Johnson, which was calculated including relativistic effects.

To treat the Sternheimer antishielding of fluorine ions in solid compounds in a more systematic manner, we analyzed nuclear quadrupole coupling data of fluor-compounds of transition metals which were derived from differential perturbed angular correlation (DPAC) measurements of the 197 keV γ -radiation emitted in the decay of the $I = 5/2$ excited state.

Nuclear quadrupole coupling data of fluorides with rutile structure (NiF₂, CoF₂, FeF₂, MnF₂) which were previously reported¹⁰ and of the perovskite RbMnF₃¹¹ were completed by DPAC-measurements of the fluorides KNiF₃, KCoF₃ and KMnF₃ with perovskite structure. There are some advantages to dealing with these classes of compounds:

i) The regular or nearly regular octahedrons in these compounds differ mainly in the 3d-state occupation of the central ion.



Dieses Werk wurde im Jahr 2013 vom Verlag Zeitschrift für Naturforschung in Zusammenarbeit mit der Max-Planck-Gesellschaft zur Förderung der Wissenschaften e.V. digitalisiert und unter folgender Lizenz veröffentlicht: Creative Commons Namensnennung-Keine Bearbeitung 3.0 Deutschland Lizenz.

Zum 01.01.2015 ist eine Anpassung der Lizenzbedingungen (Entfall der Creative Commons Lizenzbedingung „Keine Bearbeitung“) beabsichtigt, um eine Nachnutzung auch im Rahmen zukünftiger wissenschaftlicher Nutzungsformen zu ermöglichen.

This work has been digitalized and published in 2013 by Verlag Zeitschrift für Naturforschung in cooperation with the Max Planck Society for the Advancement of Science under a Creative Commons Attribution-NoDerivs 3.0 Germany License.

On 01.01.2015 it is planned to change the License Conditions (the removal of the Creative Commons License condition “no derivative works”). This is to allow reuse in the area of future scientific usage.

ii) Thus σ - and π -covalency can be treated in a first approximation as due to charge transfer from the ligand 2p-orbitals into the metal 3d-orbital and expressed by the admixture coefficients of the LCAO antibonding wave functions derived for octahedral complexes. Therefore the contribution to the EFG at the site of the fluorine-ion due to σ - and π -covalency as treated by Townes and Dailey¹⁻³ can be estimated by comparison with measurements of the fraction of unpaired spin of the fluorine 2p-orbitals by magnetic transferred hyperfine interactions (THFI)^{12, 13}.

iii) The published crystallographic data of the crystals used make it possible to estimate the lattice contribution to the EFG by a simple point-charge model.

By discussing the various contributions to the EFG we try to come to a more realistic understanding of the Sternheimer antishielding effect.

II. Experimental

The measurements were carried out with the pulsed proton beam (1 ns duration) of a KN 4000 van de Graaff-accelerator. The experimental setup is described in detail elsewhere¹⁰. Bombarding ¹⁹F with 3.5 MeV protons the 5/2⁺ level of the fluorine nucleus is excited by the (pp')-reaction and decays with a mean-life $\tau = 125$ ns by γ -ray emission. Neglecting the experimental time-resolution, the decay-curve of the γ -radiation is given by

$$N(\theta, t) = N_0 \cdot e^{-t/\tau} [1 + a_2 g_{22}(t) \cdot P_2(\cos \theta)]. \quad (1)$$

a_2 is the anisotropy of the γ -radiation and $g_{22}(t)$ is the time-dependent attenuation coefficient, which contains the information about the nuclear moment interaction with surrounding fields during the lifetime of the excited nucleus.

In the case of pure electric quadrupole-interaction, $I = 5/2$ and polycrystalline target material, $g_{22}(t)$ has the form

$$g_{22}(t) = \alpha_0 + \sum_{i=1}^3 \alpha_i \cos \omega_i t,$$

where α_0 , α_i and ω_i depend on the nuclear quadrupole moment Q and the EFG at the position of the excited nucleus, which is usually represented by the main tensor component V_{zz} given by

$$|V_{zz}| = \frac{2 I (2 I - 1)}{3 e Q} \omega_1$$

and the asymmetry-parameter η defined by

$$\eta = \frac{V_{xx} - V_{yy}}{V_{zz}}, \quad 0 \leq \eta \leq 1.$$

Because of the Laplace equation $\Delta V = 0$ one gets

$$V_{xx} = -\frac{1}{2}(1 - \eta) V_{zz},$$

$$V_{yy} = -\frac{1}{2}(1 + \eta) V_{zz}.$$

In Fig. 1 the dependence of the frequencies ω_i on η is shown. In Fig. 2a, b typical attenuation coefficients as a function of time are shown for NiF₂ and KNiF₃.

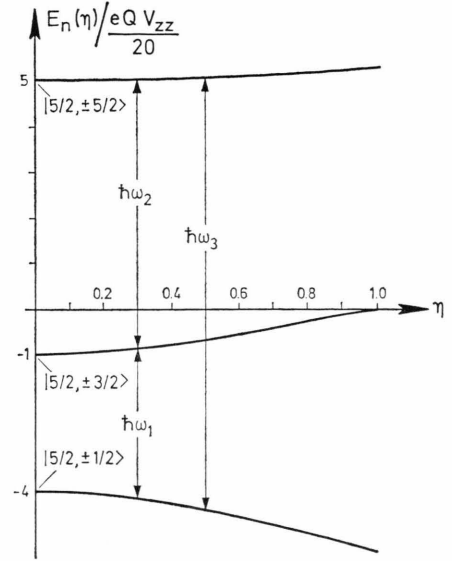


Fig. 1. Energy eigenvalues of the static quadrupole interaction Hamiltonian for $I = 5/2$ as a function of the asymmetryparameter η .

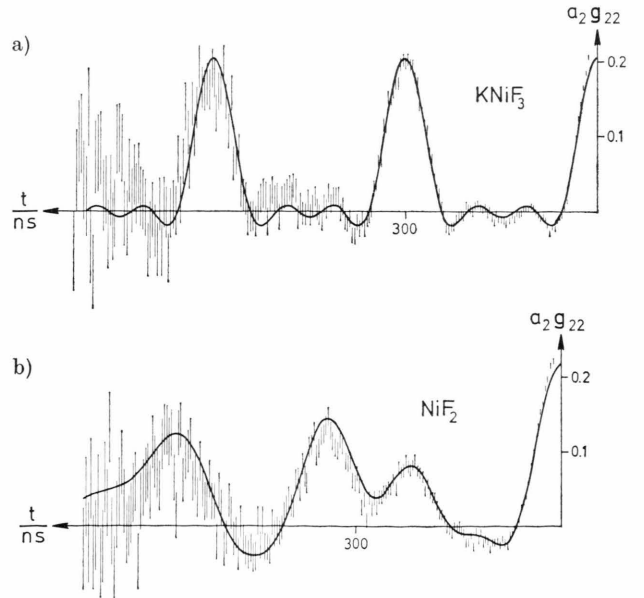


Fig. 2. Time dependent attenuation coefficient $g_{22}(t)$ for polycrystalline fluor-complexes. a) KNiF₃, b) NiF₂.

By fitting the experimental curves according to expression (1) the parameters $|V_{zz}|$ and η can be determined if the nuclear quadrupole moment Q is known. For further discussion we use the value $Q(^{19}\text{F}, 197 \text{ keV}) = 0.12 \text{ barn}$, given by Sugimoto et al.¹⁴.

The compounds with perovskite structure KNiF_3 , KCoF_3 and KMnF_3 were made as described by Rüdorff et al.^{15,16}. The lattice parameters derived from Debye-Scherrer photographs were found to be within published values¹⁷.

III. Theory

The EFG (V_{ij}^N) at a nucleus is usually expressed as a sum of an ionic contribution (V_{ij}^{ion}) and a covalent contribution (V_{ij}^{cov}) due to the covalent bounds with the nearest neighbours:

$$(V_{ij}^N) = (V_{ij}^{\text{ion}}) + (V_{ij}^{\text{cov}}) \\ = i(1 - \gamma_\infty) V_{ij}^{\text{lat}} + \sum_k w_k q_k^{\text{cov}}. \quad (2)$$

In this equation the Sternheimer antishielding $(1 - \gamma_\infty)$ is assumed to be a scalar factor; i is the ionicity and w_k means the probability for a F^- -ion to form a covalent bond with the k th nearest neighbour ($\sum w_k = 1$; bond switching model³).

q_k^{cov} is the principal component of the axially symmetric EFG due to the covalent bond directed to the k th bond axis which can be expressed in the Townes-Dailey approach for two atomic molecules as proportional to the atomic EFG q^{at} arising from the 2p-hole in the neutral fluorine atom^{2,3}:

$$q_k^{\text{cov}} = f \cdot q^{\text{at}}. \quad (3)$$

Thus the covalency factor f means the deviation of the 2p electronic charge distribution due to the charge transfer with adjacent ions from spherical symmetry. While σ -electrons transferred to the k th neighbour contribute positively to f , the transferred π -electrons, moving on the two orbitals orthogonal to the bond axis, enter negatively in f because of the Laplace-equation $\Delta V = 0$.

If we restrict ourselves to regular octahedral complexes of transition metals and neglect sp-hybridisation which is justified by theoretical and experimental arguments^{12,13,19}, the covalency factor f of Eq. (3) due to $2p \rightarrow 3d$ electron transfer can be expressed most conveniently in terms of holes in the antibonding molecular orbitals using the LCAO-MO-method. The five antibonding orbitals for octahedral complexes with e_g - and t_{2g} -symmetry are^{12,13}:

$$\begin{aligned} \psi(e_g) &= \frac{1}{\sqrt{N_\sigma}} \left\{ d_{3z^2-r^2} - \frac{\lambda_\sigma}{\sqrt{12}} (-2z_3 + 2z_6 + x_1 - x_4 + y_2 - y_5) \right\}, \\ \psi(e'_g) &= \frac{1}{\sqrt{N_\sigma}} \left\{ d_{x^2-y^2} - \frac{\lambda_\sigma}{2} (-x_1 + x_4 + y_2 - y_5) \right\}, \\ \psi(t_{2g}) &= \frac{1}{\sqrt{N_\pi}} \left\{ d_{xy} - \frac{\lambda_\pi}{2} (y_1 - y_4 + x_2 - x_5) \right\}, \\ \psi(t'_{2g}) &= \frac{1}{\sqrt{N_\pi}} \left\{ d_{yz} - \frac{\lambda_\pi}{2} (z_2 - z_5 + y_3 - y_6) \right\}, \\ \psi(t''_{2g}) &= \frac{1}{\sqrt{N_\pi}} \left\{ d_{zx} - \frac{\lambda_\pi}{2} (x_3 - x_6 + z_1 - z_4) \right\}. \end{aligned} \quad (4)$$

x , y and z represent the ligand 2p-orbitals; the index numbers 1, 2, 3, 4, 5, 6 refer to the ligands located at the x , y , z , $-x$, $-y$, $-z$ axes of the octahedron. λ_σ and λ_π are the admixture coefficients of the orbitals with e_g - and t_{2g} -symmetry. The normalization factors $N_{\sigma,\pi}$ are given by

$$N_{\sigma,\pi} = 1 - 2\lambda_{\sigma,\pi} S_{\sigma,\pi} + \lambda_{\sigma,\pi}^2,$$

where the overlap integrals $S_{\sigma,\pi}$ are:

$$S_\sigma = -2 \langle d_{x^2-y^2} | p_\sigma \rangle \quad \text{and} \quad S_\pi = 2 \langle d_{xy} | p_\pi \rangle.$$

It is customary to express the electronic charge transferred to the central ion for singly occupied e_g - and t_{2g} -orbitals in terms of fractional occupations which are, from Equation (4):

$$f_\sigma = \frac{\lambda_\sigma^2}{3N_\sigma}, \quad f_\pi = \frac{\lambda_\pi^2}{4N_\pi}. \quad (5)$$

* $q^{\text{at}} = \frac{e}{4\pi\epsilon_0} \frac{4}{5} \langle r^{-3} \rangle_{2p} = -5.1 \cdot 10^{18} \text{ V/cm}^2$ taking $\langle r^{-3} \rangle_{2p}$ from Barnes and Smith^{2,18}.

From Eq. (5) it is obvious that the corresponding charge transfers C_σ and C_π to the central ion being in an $e_g^n t_{2g}^m$ -state are²⁰:

$$\begin{aligned} C_\sigma &= (2 - n/2) f_\sigma e, \\ C_\pi &= 2(2 - m/3) f_\pi e; \end{aligned} \quad (6)$$

$(2 - n/2)$ and $(2 - m/3)$ are the number of e_g - and t_{2g} -holes respectively. The expectation value of the EFG operator q^{op} at a ligand nucleus due to its 2p-hole wave function is:

$$\langle 2p_\sigma\text{-hole} | q^{\text{op}} | 2p_\sigma\text{-hole} \rangle = q^{\text{at}},$$

and

$$2 \langle 2p_\pi\text{-hole} | q^{\text{op}} | 2p_\pi\text{-hole} \rangle = -q^{\text{at}}. \quad (7)$$

Thus we can write the EFG at the nucleus of a ligand due to the covalent $2p \rightarrow 3d$ charge transfer to the central ion in an octahedral complex as¹²

$$q^{\text{cov}} = \{(2 - n/2) f_\sigma - (2 - m/3) f_\pi\} q^{\text{at}}. \quad (8)$$

q^{cov} is the principal component of the axially symmetric covalent EFG directed to the bond axis. The curled bracket stands for the covalence factor f [see Equation (3)].

In octahedral d^8 -complexes ($t_{2g}^6 e_g^2$) where symmetry considerations do not allow π -electron transfer, the covalency factor f is reduced to f_σ ; in d^5 -complexes ($t_{2g}^3 e_g^2$) f will be given by $f_\sigma - f_\pi$. In these cases the covalency factor f arising from aspherical charge transfer can be compared in a first approximation with the fraction $f' = f_\sigma' - f_\pi'$ of unpaired spin in the ligand 2p-orbital which is known from THFI-measurements¹³ (see Table 2).

Table 2. Spin transfer coefficients from THFI-measurements.

Complex	Host lattice	$(f_\sigma' - f_\pi')/100$	Method	Ref.
$(\text{MnF}_6)^{4-}$	KMnF ₃	0.18 ± 0.1	NMR	21
	KMnF ₃	0.35 ± 0.05	NMR	22
	RbMnF ₃	0.33 ± 0.18	NMR	23
$(\text{NiF}_6)^{4-}$	KMgF ₃	3.1 ± 0.1	ESR	24
	KNiF ₃	3.78 ± 0.2	NMR	25
	NiF ₂ *	4.1 ± 0.4	NMR	26
		4.5 ± 0.4		

* The two values refer to the two different types of bond in NiF₂.

According to Tab. 2, f' from THFI-data is about 4% for $(\text{NiF}_6)^{4-}$ and is nearly zero for $(\text{MnF}_6)^{4-}$. Taking into account the $2p_\sigma \rightarrow 4s$ spin transfer which is opposite the $2p \rightarrow 3d_\sigma$ spin transfer and

therefore lowers the effective f_σ' -value for $(\text{MnF}_6)^{4-}$,¹³ $f(\text{MnF}_6^{4-}) = 1\%$, $f(\text{FeF}_6^{4-}) = 2\%$, $f(\text{CoF}_6^{4-}) = 3\%$ and $f(\text{NiF}_6^{4-}) = 4\%$ are reasonable values for our purpose, considering the decreasing π -electron transfer from $(\text{MnF}_6)^{4-}$ to $(\text{NiF}_6)^{4-}$.

The lattice EFG (V_{ij}^{lat}) of Eq. (2) can be calculated by summing the individual contributions to the EFG of all the surrounding ions. Since dipole moments of the electronic charge distribution of the surrounding ions do not exist for the metal ions (because of the inversion symmetry of the metal positions) or are negligible for the fluorine ions, (V_{ij}^{lat}) is given by a simple point-charge model:

$$(V_{ij}^{\text{lat}}) = \frac{1}{4\pi\epsilon_0} \sum_B e_B \cdot \frac{x_i^B x_j^B - r_B^2 \delta_{ij}}{r_B^5} \quad (9)$$

where B denotes the considered ion and e_B its effective point-charge. The prime indicates the omitted fluor-charge at the origin. x_i^B and r_B are the coordinates and the distance of the B-th ion. We have performed these calculations by a planewise summation method similar to that developed by de Wette and Schacher²⁷.

Following Owen et al.²⁰ who assumed that the electron charge transfer from fluorine ligands to the metal ion in octahedral transition metal complexes, which are in the same valence state, is approximately the same, the effective charges of the metal ions which enter (V_{ij}^{lat}) in Eq. (8) can be estimated from the charge transfer in $(\text{NiF}_6)^{4-}$. With $f_\sigma = 0.04$ we find

$$e_{\text{eff}}(\text{Ni}^{2+}) = (2 - 6f_\sigma) |e| = 1.76 \cdot |e|. \quad (10)$$

The still open parameters of Eq. (2) are the ionicity i and the probability factors w_k , to which we will refer in the next section.

IV. Discussion

KNiF₃, KCoF₃, KMnF₃ and RbMnF₃ crystallize in the cubic perovskite structure. The edges of a cube are occupied by the K⁺- and Rb⁺-ions respectively. The metal ion located at the body-centered position of the unit cell is surrounded by six F⁻-ions located at the face-centered positions (D_{4h} -symmetry) forming a regular MeF_6 -octahedron. Since each F⁻-ion is collinear and equal in distance with the two nearest neighbours, the probability factors w_1 and w_2 are equal and we have, according to Eqs. (2) and (3):

$$V_{zz}^{\text{cov}} = f q^{\text{at}}, \quad \eta^{\text{cov}} = 0. \quad (11)$$

Table 3. Crystallographic data of difluorides with rutile structure.

Compound	$a_0/10^{-8}$ cm *	$c_0/10^{-8}$ cm *	u **	$\overline{4} \text{ MeF}/10^{-8}$ cm	$\overline{2} \text{ MeF}/10^{-8}$ cm
NiF ₂	4.6506 (2)	3.0836 (4)	.304 (2)	2.010 (9)	1.999 (14)
CoF ₂	4.6951 (2)	3.1796 (3)	.307 (2)	2.042 (8)	2.038 (14)
FeF ₂	4.6966 (2)	3.3091 (1)	.300 (2)	2.122 (8)	1.993 (14)
MnF ₂	4.8734 (2)	3.3099 (5)	.307 (2)	2.123 (9)	2.116 (14)

* Ref.²⁸.** Ref.²⁹.

z is directed to the bond axis which coincides with the 4-fold rotation axis of the F⁻-position. Therefore the principal axes of (V_{ij}^{lat}), (V_{ij}^{cov}) and (V_{ij}^{N}) are identical and the asymmetry parameters η^{lat} , η^{cov} and η^{N} are zero which is verified by our calculations and measurements. Thus we have from Eq. (2) and (11):

$$i(1 - \gamma_{\infty}) = (V_{zz}^{\text{N}} - f q^{\text{at}})/V_{zz}^{\text{lat}}. \quad (12)$$

The compounds MnF₂, FeF₂, CoF₂ and NiF₂ have the tetragonal rutile unit cell belonging to the space-group D_{4h}^{14} which is shown in Figure 3a. Each metal ion located at (0, 0, 0) and (1/2, 1/2, 1/2) is surrounded by a slightly distorted octahedron (orthorhombic symmetry) of six F⁻-ions located at $\pm(u, u, 0)$ and $\pm(u + 1/2, 1/2 - u, 1/2)$, four of them being at a slightly different distance from the other two. The crystallographic data and the metal fluorine distances are listed in Table 3.

The principal axes of (V_{ij}^{lat}), (V_{ij}^{cov}) and (V_{ij}^{N}) are determined by the two orthogonal mirror planes of the fluorine position (Figure 3b). Each fluorine ion has three nearest neighbouring metal ions lying in the x - y -plane (Figure 4). Since two metal ions (Me₁ and Me₂) are the same distance from the fluorine and since $\sum w_k = 1$, one has: $w_1 = w_2 = w$;

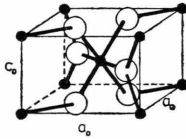


Fig. 3a. Rutile unit cell.

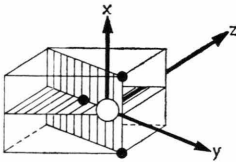


Fig. 3b. Mirror planes through the fluor position (large circle) in rutil complexes. The axes x , y and z refer to the principal axes derived from the calculations of (V_{ij}^{lat}).

$w_3 = 1 - 2w$. Thus according to Eq. (2) and (3) the covalent EFG (V_{ij}^{cov}) due to the bond with the three nearest neighbours is given by (see Figure 4):

$$\begin{aligned} V_{zz}^{\text{cov}} &= -\frac{1}{2} f q^{\text{at}}, \\ \eta^{\text{cov}} &= 3 - 12w \sin^2 \theta/2. \end{aligned} \quad (13)$$

V_{zz}^{cov} is independent of w , i.e. of the distortion of the MeF₆-octahedrons. In comparison with Eq. (10) we deduce from Eq. (2) and (13):

$$i(1 - \gamma_{\infty}) = (V_{zz}^{\text{N}} + \frac{1}{2} f q^{\text{at}})/V_{zz}^{\text{lat}}. \quad (14)$$

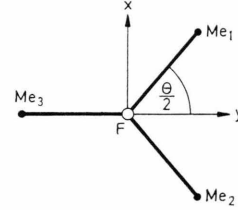


Fig. 4. The three nearest neighbors to the F⁻ ion in the x - y -plane of Figure 3b.

Because the sign of V_{zz}^{N} is not determined from DPAC-measurements with polycrystalline target material and since $(1 - \gamma_{\infty})$ is positive, the same sign for V_{zz}^{N} and V_{zz}^{lat} can be deduced from Eq. (12) and (14) (see Table 4). The contributions to Eq. (12) and (14) for the various compounds are listed in Table 4. The experimental errors are given in brackets. Since Q and q^{at} enter $i(1 - \gamma_{\infty})$ only as scaling factor, their possible errors are not taken into account. V_{zz}^{lat} were calculated using the same effective charge $e_{\text{eff}}(\text{metal}) = 1.76|e|$ for all metal ions (see Section III). Assuming

$$e_{\text{eff}}(\text{F}^-) = -e_{\text{eff}}(\text{K}^+, \text{Rb}^+) *,$$

all effective charges are determined because of charge neutrality. If we assume further, that the ionicity i is approximately the same for the listed

* A higher effective charge for the alkali ions does not change the following conclusions.

Table 4. Sternheimer antishielding factors of F^- in octohedral transition metal complexes derived from DPAC-measurements.

Complex	Compound	$\frac{eQ V_{zz} }{h}$ Mc/s	$\frac{ V_{zz}^N }{10^{18} \text{ V/cm}^2}$	$\frac{V_{zz}^{\text{lat}}}{10^{18} \text{ V/cm}^2}$	f^{**}	$i(1-\gamma_\infty)$	$\frac{\overline{\text{MeF}}}{10^{-8} \text{ cm}}$
$(\text{NiF}_6)^{4-}$	KNiF_3	21.6 (2)	0.74 (1)	0.084	0.04	11.2	2.00 ₆
$d^8(t_{2g}^6 e_g^2)$	NiF_2^{a}	18.8 (3)	0.65 (1)	− 0.076		9.9	2.00 ₆ *
$(\text{CoF}_6)^{4-}$	KCoF_3	17.9 (2)	0.62 (1)	0.081	0.03	9.5	2.03 ₅
$d^7(t_{2g}^5 e_g^2)$	CoF_2^{a}	15.2 (3)	0.52 (1)	− 0.071		8.4	2.04 ₁ *
$(\text{FeF}_6)^{4-}$	FeF_2	12.6 (3)	0.43 (1)	− 0.068	0.02	7.1	2.05 ₉ *
$d^6(t_{2g}^4 e_g^2)$							
$(\text{MnF}_6)^{4-}$	KMnF_3	11.6 (2)	0.40 (1)	0.074	0.01	6.1	2.09 ₃
	$\text{RbMnF}_3^{\text{b}}$	12.8 (2)	0.44 (1)	0.071		6.9	2.12 ₀
$d^5(t_{2g}^3 e_g^2)$	MnF_2^{a}	11.0 (3)	0.38 (1)	− 0.064		6.4	2.12 ₁ *

^a Richter, Wiegandt¹⁰; ^b private communication¹¹.

* mean value due to the nearest neighbors (see Tab. 3)

** assumed values (see Section III).

Tab. 5. Overlap integrals for $(\text{MeF}_6)^{4-}$ complexes with Me-F-seperation of 2.01 Å (Ref. ³⁰).

Central Ion	S_σ	S_π	S_s
$d^8 \text{ Ni}^{2+}$	0.104	0.078	0.088
$d^7 \text{ Co}^{2+}$	0.114	0.087	0.099
$d^6 \text{ Fe}^{2+}$	0.125	0.095	0.108
$d^5 \text{ Mn}^{2+}$	0.135	0.104	0.119

compounds, the values for $i(1-\gamma_\infty)$ give the relative significance of the Sternheimer antishielding.

In Table 4 the increasing antishielding with increasing 3d occupancy of the metals both for perovskite and rutile fluorides is obvious. This may

be further reinforced by the increasing Me-F distances as indicated in the case of KMnF_3 and RbMnF_3 , since the Me-F distance decreases from complexes with d^5 - to complexes with d^8 -ions. This trend is highly correlated with the overlap integrals of these complexes which were calculated by Davies et al.³⁰ using Clementi's wave functions (Table 5).

The differences between the antishielding factors of F^- in fluorides with perovskite and rutile structure arise, in our opinion, mainly for two reasons:

Firstly the influence to the EFG of the electric field (of the order of 10^8 V/cm , see Table 6) at the fluorine position in rutile fluorides has to be taken

Comp.	NiF_2	CoF_2	FeF_2	MnF_2
$\frac{E}{V/10^{-8} \text{ cm}}$	− 0.90 (12)	− 0.76 (11)	0.14 (12)	− 0.67 (10)

Table 6. Point-charge calculation of the electric field at the fluorine position in rutile fluorides directed to the y -axis of Figure 4.Table 7. Comparison of the asymmetryparameter η^N (from measurement), η^{lat} (point-charge calculation) and η^{cov} [Eq. (13)]. The errors of η^{lat} and η^{cov} are due to the errors of the fluorine position parameter μ (Table 3). * See Figure 4.

Comp.	η^N	η^{lat}	η^{cov}			$\sin^2 \theta/2^*$
			$(w = 0.30)$	$(w = 1/3)$	$(w = 0.35)$	
NiF_2	0.44 (3)	0.61 (6)	0.88 (2)	0.64 (2)	0.53 (2)	0.589 (5)
CoF_2	0.48 (3)	0.51 (6)	0.82 (2)	0.57 (2)	0.46 (2)	0.606 (5)
FeF_2	0.47 (3)	0.72 (6)	0.81 (2)	0.57 (2)	0.45 (2)	0.608 (5)
MnF_2	0.40 (3)	0.51 (6)	0.81 (2)	0.57 (2)	0.45 (2)	0.608 (5)

into consideration, which may arise — following Dixon and Bloembergen — from mixing of bonding and antibonding orbitals^{31–33}. Since the influence to the EFG caused by an electric field is then opposite in sign for σ - and π -electrons, i.e. increases with decreasing π -electron transfer, it seems to be understandable from Eq. (12) and (14) that the antishielding factors for MnF_2 and RbMnF_3 do not disagree very much in contrary to the antishielding factors for CoF_2 , KCoF_3 and NiF_2 , KNiF_3 respectively (see Table 4).

Further, one has to ask whether the concept of a scalar antishielding factor is realistic in systems where the external EFG is of less than axial symmetry. Comparing the measured and calculated

asymmetry parameters for the rutile fluorides which are listed in Table 7, it seems necessary to assume anisotropic antishielding. The asymmetry parameters η^{cov} due to the covalent contribution to the EFG were calculated according to Eq. (13) using three values for the probability factor w : $w = 0.30$; $w = 1/3$; $w = 0.35$. (Since the three nearest neighbours are nearly equal in distance — see Fig. 4, Table 3 — w is assumed to be about $1/3$.) As can be seen from Table 7, it is not possible to satisfy Eq. (2) for all components of the EFG (V_{ij}^N) and thus to describe the antishielding effect by a scalar factor only. In comparison to isotropic shielding, anisotropic shielding may change V_{zz}^N and η^N up to 25%, as was estimated by Stout and Garret³⁴.

- ¹ E. A. C. Lucken, Nuclear Quadrupole Coupling Constants. Academic Press, London-New York 1969.
- ² C. H. Townes and A. L. Schawlow, Microwave Spectroscopy. McGraw-Hill Book Company, Inc. New York 1955.
- ³ T. P. Das and E. L. Hahn, Nuclear Quadrupole Resonance Spectroscopy. Solid State Physics Suppl. 1, Academic Press, New York-London 1958.
- ⁴ E. H. Carlson and H. S. Adams, J. Chem. Phys. **51**, 388 [1969].
- ⁵ R. G. Barnes, S. L. Segel, and W. H. Jones Jr., J. Appl. Phys. Suppl. to Vol. **33**, 269 [1962].
- ⁶ A. Narath, Phys. Rev. **136**, A 766 [1964]; Phys. Rev. **140**, A 552 [1965].
- ⁷ D. V. G. L. Narasimha Rao and A. Narasimhamurthy, Phys. Rev. **132**, 961 [1963].
- ⁸ B. Morosin and A. Narath, J. Chem. Phys. **40**, 1958 [1964].
- ⁹ F. D. Feiock and W. R. Johnson, Phys. Rev. **187**, 39 [1969].
- ¹⁰ F. W. Richter and D. Wiegandt: Z. Phys. **217**, 225 [1968].
- ¹¹ H. Haas, private communication.
- ¹² R. Bersohn and R. G. Shulman, J. Chem. Phys. **45**, 2298 [1966].
- ¹³ J. Owen and J. H. M. Thornley, Rep. Progr. Phys. **29**, 675 [1966].
- ¹⁴ K. Sugimoto, A. Mizobuchi, and K. Nakai, Phys. Rev. **134**, B 539 [1964].
- ¹⁵ W. Rüdorff, J. Kändler, and D. Babel, Z. Anorg. Chem. **317**, 261 [1962].
- ¹⁶ W. Rüdorff, G. Linke, and D. Babel, Z. Anorg. Chem. **320**, 150 [1963].
- ¹⁷ D. Babel, Structure and Bonding Vol. 3. Springer-Verlag, Berlin 1967.
- ¹⁸ R. G. Barnes and W. V. Smith, Phys. Rev. **93**, 95 [1954].
- ¹⁹ M. A. Whitehead and H. H. Jaffé, Trans. Faraday Soc. **57**, 1884 [1961].
- ²⁰ J. Owen, J. A. M. Thornley, and C. G. Windsor, Proc. Phys. Soc. **85**, 103 [1965].
- ²¹ R. G. Shulman and K. Knox, Phys. Rev. **119**, 94 [1960].
- ²² K. Egashira and K. Hirakawa, J. Phys. Soc. Jap. **22**, 344 [1967].
- ²³ M. B. Walker and R. W. H. Stevenson, Proc. Phys. Soc. **87**, 35 [1966].
- ²⁴ T. P. P. Hall, W. Hayes, R. W. H. Stevenson, and J. Wilkens, J. Chem. Phys. **38**, 1977 [1963].
- ²⁵ R. G. Shulman and S. Sugano, Phys. Rev. **130**, 506 [1963].
- ²⁶ R. G. Shulman, Phys. Rev. **121**, 125 [1961].
- ²⁷ F. W. de Wette and G. E. Schacher, Phys. Rev. **137**, A 78 [1965].
- ²⁸ W. H. Baur, Naturwiss. **12**, 349 [1957].
- ²⁹ J. W. Stout and R. G. Shulman, Phys. Rev. **118**, 1136 [1960].
- ³⁰ J. J. Davies, S. R. P. Smith, J. Owen, and B. F. Hann, J. Phys. C **5**, 245 [1972].
- ³¹ R. W. Dixon and N. Bloembergen, J. Chem. Phys. **41**, 1739 [1964].
- ³² J. Pontnau and R. Adde, Phys. Rev. **B 14**, 3778 [1976].
- ³³ D. L. Lyfar, V. E. Goncharuk and S. M. Ryabchenko, phys. stat. sol. (b) **76**, 183 [1976].
- ³⁴ E. W. Stout Jr. and B. B. Garrett, J. Chem. Phys. **59**, 3604 [1973].